The Localization of Myosin VI at the Golgi Complex and Leading Edge of Fibroblasts and Its Phosphorylation and Recruitment into Membrane Ruffles of A431 Cells after Growth Factor Stimulation

Folma Buss,* John Kendrick-Jones,‡ Corinne Lionne,‡ Alex E. Knight,‡ Graham P. Côté,§ and J. Paul Luzio*

*Department of Clinical Biochemistry, University of Cambridge, Addenbrooke's Hospital, Cambridge, CB2 2QR, United Kingdom; ‡MRC Laboratory of Molecular Biology, Cambridge CB2 2QH, United Kingdom; and §Department of Biochemistry, Queens University, Kingston, Ontario K7L 3N6, Canada

Abstract. Myosin VI is an unconventional myosin that may play a role in vesicular membrane traffic through actin rich regions of the cytoplasm in eukaryotic cells. In this study we have cloned and sequenced a cDNA encoding a chicken intestinal brush border myosin VI. Polyclonal antisera were raised to bacterially expressed fragments of this myosin VI. The affinity purified antibodies were highly specific for myosin VI by immunoblotting and immunoprecipitation and were used to study the localization of the protein by immunofluorescence and immunoelectron microscopy. It was found that in NRK and A431 cells, myosin VI was associated with both the Golgi complex and the leading, ruffling edge of the cell as well as being present in a cytosolic pool. In A431 cells in which cell surface ruffling was stimulated by EGF, myosin VI was phosphorylated and recruited into the newly formed ruffles along with ezrin and myosin V. In vitro experiments suggested that a p21-activated kinase (PAK) might be the kinase responsible for phosphorylation in the motor domain. These results strongly support a role for myosin VI in membrane traffic on secretory and endocytic pathways.

Key words: myosin • actin • cytoskeleton • membranes • Golgi complex

THE intracellular position and morphology of organelles together with the movement of vesicular carriers on membrane traffic pathways are dependent on the cytoskeleton. The role of the microtubule cytoskeleton and its associated motor proteins, kinesin and dynein, in organelle organization and membrane traffic is generally accepted (for review see Cole and Lippincott-Schwartz, 1995; Allan, 1996; Goodson et al., 1997), whereas less is known about the role of the actin cytoskeleton and associated unconventional myosins. Evidence that the actin cytoskeleton is important in both the secretory and endocytic pathways has accrued over many years. The effects of agents disrupting actin filaments on regulated insulin secretion and constitutive exocytosis have long suggested a role for the cortical actin network in the secretory process (Orci et al., 1972; Li et al., 1994; Muallem et al., 1995). Partial breakdown of the network, which acts as a barrier for access to the plasma membrane, increases secretion, whereas the complete disassembly of actin filaments stops it (Muallem et al., 1995). In yeast, mutations in the actin gene *ACT1* cause an accumulation of secretory vesicles providing genetic evidence for the importance of the actin cytoskeleton in secretion (Novick and Botstein, 1985). There has also been speculation concerning a role for actin in the secretory pathway at the level of the Golgi complex because of the discovery of the actin binding proteins spectrin and comitin in the Golgi (Weiner et al., 1993; Beck et al., 1994). On endocytic pathways the importance of the actin cytoskeleton has been established both through the use of agents disrupting actin filaments and through the isolation and characterization of informative yeast mutants (Kubler and Riezman, 1993). The effects of cytochalasin D have shown the importance of the cortical actin terminal web in clathrin mediated endocytosis at the apical surface of polarized epithelial cells (Gottlieb et al.,

Dr. Knight's current address is Biology Department, University of York, Heslington, York Y01 5DD, UK.

Address correspondence to Folma Buss, Department of Clinical Biochemistry, University of Cambridge, Addenbrooke's Hospital, Hills Road, Cambridge, CB2 2QR, UK. Tel.: 44 1223 336782. Fax: 44 1223 330598. E-mail: fb1@mole.bio.cam.ac.uk

1993; Jackman et al., 1994; Shurety et al., 1996) and the use of latrunculin has given insights into its function in endocytic uptake in nonpolarized mammalian cells (Lamaze et al., 1997) and yeast (Ayscough et al., 1997). There is also a documented role for the actin cytoskeleton in phagocytic uptake (Greenberg et al., 1991) and macropinocytosis (Swanson and Watts, 1995). Three lines of evidence implicate the involvement of actin in the later steps of the endocytic pathway; first, RhoD, a small GTPase which causes rearrangements of the actin cytoskeleton, affects the mobility and distribution of early endosomes (Murphy et al., 1996); second, cytochalasin D blocks the delivery of endocytosed macromolecules to degradative compartments (Van Deurs et al., 1995; Durrbach et al., 1996), and finally, lysosome specific isoforms of ankyrin have been identified (Hoock et al., 1997).

When the actin cytoskeleton is involved, the force for vesicle budding, vesicle movement and the protrusion and retraction of membranes is believed to be generated by ATP dependent interactions of myosin motor proteins with actin. Recently, there has been an explosion in the number of myosin motor proteins identified, mainly at the DNA level, and these have been grouped into 15 different classes based on sequence analysis (Cope et al., 1996; Mermall et al., 1998; Probst et al., 1998). Members of several different classes and several members of the same class are expressed simultaneously in the same cell (Bement et al., 1994). There is evidence that members of three classes, myosin I, V, and VI are involved in membrane transport (reviewed in Hasson and Mooseker, 1995). Myosin I has been localized in polarized epithelial cells on Golgi-derived secretory vesicles and has been proposed to play a role in their movement through the terminal web (Fath and Burgess, 1993; Fath et al., 1994).

We are particularly interested in myosin VI, since preliminary evidence shows that it has the potential to play a role in vesicle movement, but little is known about the intracellular localization and function of this class of myosin. In *Drosophila* embryos, movement of cytoplasmic particles and formation of the pseudocleavage furrow was inhibited after microinjection of antibodies to myosin VI (Mermall et al., 1994; Mermall and Miller, 1995). Recently, a *Drosophila* homologue of a microtubule binding protein called D-CLIP190 was identified as a protein associated with myosin VI (Lantz and Miller, 1998). In polarized cells immunolocalization studies have shown that myosin VI is predominantly concentrated in the terminal web below the apical brush border although there is some staining also in the microvilli (Heintzelman et al., 1994). Interestingly, a myosin VI gene has recently been identified as the gene mutated in the recessive deafness disorder observed in *Snell's waltzer* mice (Avraham et al., 1995). In the sensory hair cells of the inner ear of the bullfrog myosin VI is expressed at high concentration and is localized in the cuticular plate in association with the stereocilia rootlets, suggesting that it is involved in anchoring the stereocilia in the cuticular plate (Hasson et al., 1997). In these cells it was also found to be present in the pericuticular necklace, which is the region between the cuticular plate and the circumferential actin belt that contains a large concentration of vesicles which are thought to be involved in traffic from the Golgi complex to the apical cell surface (Hasson et al., 1997). The stereocilia may restrict access to the apical surface and thus the vesicles accumulate in the pericuticular region.

In this study, we have cloned and sequenced a cDNA encoding a myosin VI from chicken intestinal brush border cells. We raised polyclonal antisera to bacterially expressed domains of this myosin VI that specifically react with this class of myosin in different species and used them to show that in two cell lines, NRK and A431, myosin VI is associated with the Golgi complex and the leading, ruffling edge of the cell as well as being present in a cytosolic pool. We provide evidence that myosin VI is phosphorylated in the motor domain and is recruited into cell surface ruffles when stimulated by EGF. In vitro experiments demonstrate that the myosin VI motor domain is phosphorylated by p21-activated kinase (PAK)[1]. We discuss the role that myosin VI may play in membrane ruffling and membrane traffic pathways.

Materials and Methods

Recombinant DNA Procedures and Cloning of Myosin VI

Standard molecular biology procedures (Sambrook et al., 1989) were performed unless otherwise stated. Wizard prep. kits (Promega, Southampton, UK) were used for high purity plasmid isolation and Qiaex II kits (QIAGEN, Chatsworth, CA) for purification of DNA from agarose gels. The myosin VI cDNA was isolated from a chicken intestine brush border cDNA library in λgt10 kindly provided by Dr. Paul Matsudaira (MIT, Cambridge, MA) using a PCR-based strategy. A degenerate primer for the highly conserved sequence of the phosphate binding loop in the myosin ATP-binding site (GESGAGKT) was designed and used in PCR reactions together with a pair of primers which annealed either side of the multiple cloning site in the vector (Knight and Kendrick-Jones, 1993). The PCR products were cloned into the plasmid vector pTZ18R and sequenced. One of the clones with a potential open reading frame encoding a myosin-like sequence was selected and the insert used as a probe to screen the original chicken cDNA library in order to isolate a full-length cDNA encoding myosin VI. Three clones of 1.5, 2.5, and 4 kb were isolated and partially sequenced using the Sequenase sequencing kit according to the manufacturer's instructions (USB/ Amersham, Little Chalfont, UK). The DNA sequence was completed and confirmed by dideoxy chain termination sequencing, using the service provided by Oswel (Southampton, UK).

Preparation of Myosin VI Fusion Proteins and Antibodies to Myosin VI

Restriction fragments of the full-length (4 kb) myosin VI cDNA clone corresponding to different predicted domains of the molecule were cloned into pGEX (Pharmacia, St. Albans, UK) to create glutathione-*S*-transferase (GST) fusion proteins or into pRSET (Invitrogen, Leek, Holland) to express proteins with six extra histidine residues i.e., a His tag, added at the NH_2 terminus. These were: (*a*) a BamHI-fragment encoding amino acids (aa) 308–631 of the NH_2-terminal head (motor) domain, (*b*) a HindIII-fragment encoding aa 742–1,030 covering the spacer region, the IQ motif and the coiled-coil domain of the myosin VI tail, (*c*) a PstI-fragment encoding the COOH-terminal predicted globular domain from aa 1,062–1,273 and (*d*) a 45-kD fragment encoding aa 846–1,254 of the whole tail domain amplified by PCR using a set of primers containing EcoRI/BamHI restriction sites. Each of the pGEX- or pRSET-constructs was sequenced before expression in *Escherichia coli* BL 21 (DE3) cells (Studier and Moffat, 1986). To express GST-fusion proteins, freshly transformed single colo-

1. *Abbreviations used in this paper:* aa, amino acid; ab, antibody; GST, glutathione-*S*-transferase; His, Histidine; MIHCK, myosin I heavy chain kinases; MPR, cation-independent mannose 6-phosphate receptor; PAK, p21-activated protein kinase; PGT, globular tail ab.

nies were grown overnight at 37°C in 10 ml of 2× trypto yeast medium containing 0.1 mg/ml ampicillin and then diluted the next day into 1 liter of 2× trypto yeast medium containing 0.1 mg/ml ampicillin and grown to an A_{600} of 0.5–0.6 before induction by addition of isopropyl β-D-thiogalacto-pyranoside to 0.4 mM. After growing for an additional 3 h at 37°C, the cells were harvested and lysed by sonication in 25 mm Tris-HCl, pH 8.0, containing 1 mM EGTA, 1 mM DTT, 1% Triton X-100, and a protease inhibitor cocktail (complete™; Boehringer Mannheim, Lewes, UK). Approximately 80% of the coiled coil tail and ~50% of the predicted globular tail GST-fusion proteins were found in the soluble supernatant after centrifugation (30,000 *g*, 10 min), but the head domain GST-fusion protein was insoluble. The soluble GST-fusion proteins were purified by ion exchange chromatography on DE 52 cellulose (Whatman, Maidstone, UK) using a 0–500 mM linear NaCl gradient prepared in the lysis buffer, followed by a glutathione–Sepharose 4B affinity column used according to the manufacturer's instructions (Pharmacia Uppsala, Sweden). Insoluble inclusion bodies containing the GST-myosin VI head domain were washed at least six times with the lysis buffer and then dissolved in 8 M urea, 25 mM Tris-HCl, pH 8.0, 1 mM EGTA, and 1 mM DTT (Nagai and Thøgersen, 1987). After clarification by centrifugation (30,000 *g*, 20 min) the protein was purified in the presence of urea by ion exchange chromatography on DE 52 as described above. Before applying the protein to the glutathione–Sepharose 4B affinity column it was renatured by first diluting the urea concentration to 4 M with 50 mM Tris-HCl, 5 mM EDTA, and 10 mM DTT, pH 8.0, leaving it to stand for 2 h at 4°C and then dialyzing against 20 mM Tris-HCl, 1 mM EDTA, 1 mM DTT, pH 8.0. The expressed proteins with the NH_2-terminal His tags were solubilized in the 8 M urea solution (above) (with in addition 500 mM NaCl and 20 mM Imidazol, pH 7.0) and purified and refolded on a Ni^{2+} agarose column (Ni-NTA-agarose, QIAGEN) i.e., the fragments were bound in the 8 M urea solution, washed in the same solution, then washed in 4 M urea, 2 M urea, 500 mM NaCl, and finally PBS. The fragments were eluted with PBS and 250 mM imidazole, pH 7.0, and stored after dialysis against 500 mM NaCl, 1 mM Mg^{2+}, 10 mM P_i, pH 7.0, and 1 mM DTT. Aliquots of 0.5 mg of the purified myosinVI fusion proteins were injected into rabbits to raise polyclonal antisera using standard techniques (Harlow and Lane, 1988). Specific antibodies were affinity purified on GST-fusion proteins and/or also on His tagged fusion proteins separated by SDS-PAGE and transferred onto nitrocellulose. Nitrocellulose strips containing these purified fusion proteins were incubated overnight at 4°C with 2 ml of antiserum that had in the case of GST fusion protein been passed through a GST-agarose affinity column (10 mg of purified GST coupled to 2ml of Aminolink™ gel; Pierce, Chester, UK) to remove any anti-GST antibodies. After incubation the nitrocellulose strips were washed extensively with PBS and specific bound antibodies eluted using 0.2 M glycine HCl, pH 2.5. After neutralization with 1 M Tris-HCl, pH 7.4, the antibodies were stored after addition of 0.1% gelatin and 0.02% sodium azide.

Preparation of a Myosin V Fusion Protein and Antibodies to Myosin V

A PstI fragment of 1,122 base pairs was excised from a clone of *Dilute* myosin V tail cDNA (gift from Dr. N. Jenkins, NCI-Frederick Cancer Research and Development Center, Frederick, Bethesda, MD), subcloned into BlueScript vector (Stratagene, Cambridge, UK) and sequenced. This fragment encoding residues 987 to 1,362 of the *Dilute* protein was subcloned, using BamHI and EcoRI restriction sites, into the expression vector pRSET. The His-tagged fusion protein was expressed in *E. coli* BL21 (DE3) cells as described for the His-tagged myosin VI fragment and was purified under denaturing conditions (8 M urea) using a Ni^{2+}-NTA-agarose resin column, according to the manufacturer instructions (QIAGEN, Chatsworth, CA).

To raise polyclonal antibodies rabbits were injected with recombinant myosin V as described for myosin VI. Specific antibodies were purified from the rabbit serum by ammonium sulfate precipitation followed by affinity purification using the appropriate fusion protein bound to an Aminolink™ gel (Pierce).

Other Antibodies

Other antibodies used in this study were: a mouse monoclonal antibody (mAb) to TGN38 (gift from Dr. G. Banting, University of Bristol, Bristol, UK), mouse mAbs to mannosidase II and GM130 (gifts from Dr. G. Warren, ICRF, London, UK), an mAb to galactosyl transferase (provided by Dr. T. Suganuma, Miyazaki Medical College, Miyazaki, Japan) and rabbit polyclonal antibodies to ezrin (gift from Dr. A. Bretscher, Cornell University, Ithaca, NY).

Affinity-purified antibodies to myr 2 (myosin I from rat brain; Ruppert et al., 1995) were prepared against expressed GST-fusion protein of the tail domain (cDNA for myr2, provided by Dr. M. Bähler, Ludwig-Maximilians-Universität, Munich, Germany).

Electrophoresis and Immunoblotting

Electrophoresis of proteins (SDS-PAGE) was carried out in 7.5–17.5% acrylamide gradient gels according to Matsudaira and Burgess (1978). The separated proteins were transferred electrophoretically to nitrocellulose sheets using a semidry blotter (Kyhse-Anderson, 1984). The proteins on the nitrocellulose were stained with 0.2% Ponceau-S in 10% acetic acid. The nitrocellulose was blocked with 5% nonfat dried milk and the blots were then incubated with the polyclonal rabbit antisera followed by goat anti–rabbit IgG coupled to alkaline phosphatase (Sigma Chemical Co., St. Louis, MO) and subsequent development of reaction product as previously described (Harlow and Lane, 1988).

Cell Culture

NRK cells (normal rat kidney fibroblasts) were obtained from the European Collection of Animal Cell Cultures and human A431 cells were provided by Dr. Colin Watts (University of Dundee, Dundee, UK). Both cell lines were grown in DME supplemented with 10% FCS and 2 mM L-glutamine. The amount of myosin VI in these cells was determined by blotting using the affinity-purified antibody to the tail domain and purified recombinant myosin VI as a standard. For EGF (GIBCO BRL, Paisley, UK) stimulation of ruffling, A431 cells were preincubated in serum-free DME containing 2 mg/ml BSA. Then 200 ng/ml EGF was added and the cells incubated for different times.

Radiolabeling of Cells and Immunoprecipitation

Radioactive labeling of cells was performed on subconfluent cultured cells grown on 90-mm plates. For the ^{33}P-labeling, A431 cells were first incubated for 1 h at 37°C in serum-free and phosphate-free medium (Sigma Chemical Co.) before adding 0.5 mCi of ^{33}P-orthophosphate (Amersham, UK) to each 90-mm plate. After further incubation for 1 h at 37°C, cells were stimulated with 200 ng/ml EGF for different times up to 15 min. Cells were then quickly washed with TBS and scraped into 1 ml of extraction buffer containing phosphatase and protease inhibitors: 25 mM Tris-HCl, pH 7.4, containing 150 mM NaCl, 1 mM EDTA, 0.1% SDS, 1% Triton X-100, 1% deoxycholate, 1 mM PMSF, a protease inhibitor cocktail (complete™, Boehringer), 1 mM Na_3VO_4, 30 mM NaF, and 10 mM $Na_2P_2O_7$. Similarly for ^{35}S-labeling, A431 and NRK cells grown on 90-mm plates were preincubated for 1 h at 37°C in methionine/cysteine-free MEM containing 5% dialysed FCS. After a brief wash with PBS, 0.2 mCi of [^{35}S]methionine/cysteine (Pro-mix; Amersham, UK) in 4 ml of methionine/cysteine free MEM supplemented with 20 mM Hepes, pH 7.4, was added to the cells and incubation continued for 1 h at 37°C. The cells were washed three times with PBS and scraped into 1 ml of extraction buffer without the phosphatase inhibitors. The cell extracts after ^{35}S- or ^{33}P-labeling were first sonicated on ice to reduce viscosity and then cleared by centrifugation at 50,000 *g* for 30 min. 200 μl of supernatant was mixed first with 20 μl of nonimmune rabbit serum and 20 μl of protein A–Sepharose beads (50 mg/ml; Sigma Chemical Co.) and incubated at 4°C for 30 min. The nonimmune complex was sedimented by centrifugation and the resultant supernatant incubated with 20 μl of the specific antiserum. After 1 h this mixture was centrifuged in a microfuge (13,000 *g*, 15 min) and the resultant supernatant mixed with 50 μl of protein A–Sepharose beads (50 mg/ml). After 1 h the immunoprecipitates were washed eight times with extraction buffer by briefly sedimenting in the microfuge, aspirating the supernatant and then resuspending the Sepharose beads again in 0.5 ml of extraction buffer. Finally the Sepharose beads was washed twice in 50 mM Tris-HCl, pH 7.4, before processing for SDS-PAGE.

For limited proteolytic cleavage of myosin VI, A431 cells were labeled as described above with ^{33}P. They were then extracted with a buffer containing 25 mM Tris-HCl, pH 7.4, 150 mM NaCl, 1 mM EDTA, protease and phosphatase inhibitors (see above), and 1% IGEPAL CA-630 (Sigma Chemical Co.) but no denaturing detergent, because digestion with chymotrypsin in the presence of SDS leads to complete cleavage to small fragments. After immunoprecipitation and washing, pellets were finally washed and resuspended in 25 mM Tris-HCl, pH 7.2, 150 mM NaCl, 1 mM

$CaCl_2$, and incubated with Chymotrypsin (Sigma Chemical Co.) at 1:200 (wt/wt) for 30 min at 25°C. The digests were then processed for SDS-PAGE.

In Vitro Phosphorylation Assay

For in vitro phosphorylation, myosin VI and myr 2 (myosin I) were immunoprecipitated from A431 cells, and the immunoprecipitates washed thoroughly, as described above. The immunoprecipitates were taken up in 20 μl kinase buffer containing 2 mM $MgCl_2$, 10 mM TES, pH 7.0, 1 mM DTT, 0.1 mg/ml BSA, 250 μM γ-[^{32}P]ATP with a specific activity of 1 μCi/nmol and 30 ng of GST-PAK (Wu et al., 1996). After 30 min at 37°C the reaction mixtures were processed for SDS-PAGE. The same conditions were used for in vitro phosphorylation of recombinant myosin VI head domain (aa 308–631), purified expressed GST and chicken smooth muscle myosin II subfragment 1.

Actin Binding Assay

Myosin VI immunoprecipitated from A431 cells on protein A–coated Sepharose beads was incubated with 10 μM F-actin in PBS containing 1 mM $MgCl_2$ and 1 mM DTT and with or without 2.5 mM MgATP. After 15 min at 4°C the beads were washed intensively by brief centrifugation (less then 10 s at 13, 000 *g*) to remove the F-actin not bound to myosin VI. Under these centrifugation conditions virtually none of the F-actin pelleted in the absence of the myosin coated beads. The same protocol was used to determine actin binding to myosin VI phosphorylated in vitro by PAK.

Preparation of Rat Liver and Rat Kidney Golgi Membranes

Golgi membranes from rat liver (40 g wet weight) were prepared by the procedure of Slusarewicz et al. (1994) with one modification. The first step gradient was run twice to reduce contamination caused by overloading the gradient. Golgi membranes from rat kidney were purified by the same method, except that a different homogenization protocol was used. 20 rat kidneys (24 g wet weight) were chopped very finely on a glassplate using sharp razor blades and then homogenized carefully by using an omnimix probe for 10 s at a medium setting (OCI Instruments, Waterbury CT).

Immunofluorescence

For immunofluorescence microscopy, cells were grown on coverslips and fixed with 4% formaldehyde in PBS for 15 min, permeabilized with 0.2% Triton X-100 for 10 min and then incubated with various first antibodies at room temperature for 1 h. The second antibody used was either a sheep anti–mouse IgG coupled to fluorescein, a donkey anti–rabbit IgG coupled to Texas red (supplied by Amersham Life Science, UK) and was added for 1 h at room temperature. After each incubation the coverslips were washed several times with PBS and 0.2% BSA. The coverslips were mounted on slides in Mowiol (Hoechst AG, Frankfurt, Germany) and analyzed and photographed using a Zeiss Axiophot microscope or a Bio-RAD MRC 1000 confocal microscope.

Immunoelectron Microscopy

Ultrastructural immunocytochemistry on frozen ultrathin sections was performed as described by Griffiths (1993) and Reaves et al. (1996) with the modification that the cells were fixed in 4% formaldehyde, 0.1% glutaraldehyde. To quantitate the labeling density on different plasma membrane areas, we counted gold particles on either unruffled stretches of plasma membrane or on membrane protrusions i.e., ruffles, filopodia and lamellipodia. Results are presented as number of gold particles per boundary length according to Griffiths (1993) and Griffiths and Hoppeler (1986).

Results

Sequence Analysis of Chicken Brush Border Myosin VI

A full-length cDNA encoding a chicken brush border myosin VI was isolated and sequenced. The amino acid sequence (Fig. 1) is 90% identical to that of pig myosin VI (Hasson and Mooseker, 1994) and 60% identical to

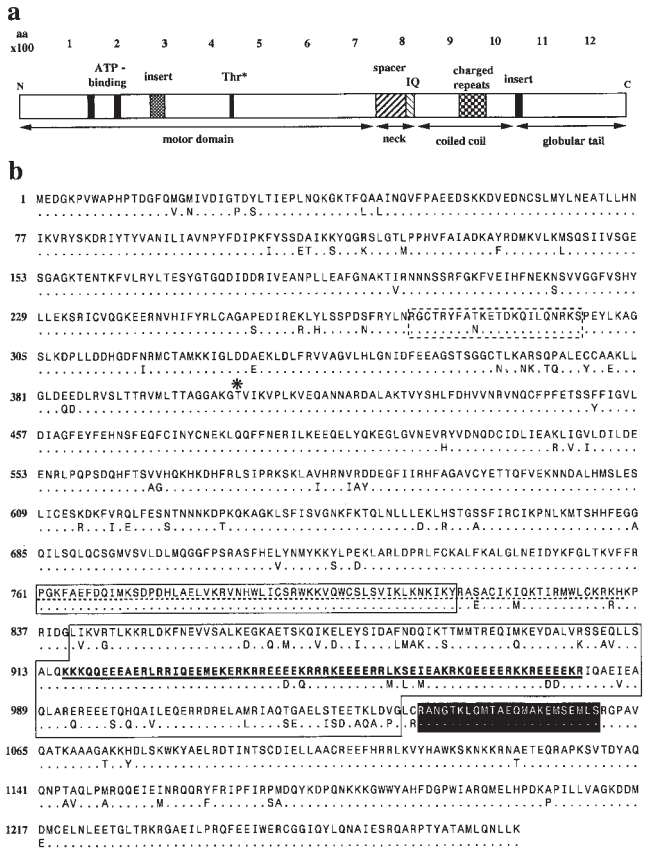

Figure 1. Amino acid sequence of the chicken brush border myosin VI. (*a*) Schematic representation of the domain organization and special features in the sequence. (*b*) Alignment of the chicken brush border myosin VI sequence (*top*) with porcine myosin VI (*bottom*). Dots indicate identical amino acids, whereas capital letters indicate a different amino acid. Features are highlighted as follows (starting from the NH_2-terminus): box surrounded by dashed line, 22 amino acid insert in the head domain; *threonine$_{406}$ a possible phosphorylation site for a specific heavy chain kinase; box surrounded by solid line with sequence dashed underlined, spacer region COOH-terminal of the motor domain; *dashed underlined*, IQ motif; *box surrounded by solid line*, region of predicted coiled coil; *bold letters* and *underlined* within this coiled coil region are charged repeats; *shaded box*, 23-aa insert in the myosin VI tail.

Drosophila 95F myosin VI (Kellerman and Miller, 1992). The chicken myosin VI has a predicted molecular mass of 147.7 kD. The amount of myosin VI present in tissue culture cells such as human epidermoid carcinoma A431 cells was estimated as 0.15% of the total protein present. All of the myosin VIs so far sequenced have a number of unique features compared with other myosins (Hasson and Mooseker, 1994). Within the motor domain there is a small insert of 22 residues (276–297). After the motor domain there is a ~53 residue spacer region with no known structural motifs (maybe it binds an unusual light chain subunit) followed by a single IQ motif which is predicted to bind calmodulin. Directly after the IQ motif there is a region predicted to form an α-helical coiled coil, both by the algorithm of Andrei Lupas (Lupas et al., 1991) and by

the Paircoil method (Berger et al., 1995). This coiled coil seems to fall into two blocks at residues 846–887 and 921–1002 (see Fig. 1). However, overlapping with the second block is a region containing several repeats of charged aa (916–981). These repeats typically consist of four basic residues followed by four acidic residues, e.g., RKRREEEE. This region is well conserved among the vertebrate myosin VI sequences and seems most unlikely to form a stable coiled coil structure. Secondary structure predictions using the nnpredict method (Kneller et al., 1990) amongst others suggest that most of these charged residues are in an alpha helix. Searching protein sequence databases for a similar sequence repeat using the PatternFind server (http://ulrec3.unil.ch/software/software.html) found very few proteins with similar repeats. It seems most likely that this structure would form a helix that is completely exposed to the aqueous environment, with alternating bands of positively and negatively charged residues on its surface which may stabilize the helix. Immediately after the end of this region there is an insertion of 23 aa in the chicken myosin VI sequence compared with the porcine myosin VI sequence (Hasson and Mooseker, 1994), which suggests that the chicken myosin VI gene maybe differentially spliced in the tail. Preliminary PCR analysis indicates that the transcript with the 23-aa insert is the major species in the chicken brush border cDNA library but both isoforms with and without the insert are present in various ratios in several vertebrate libraries screened to date (data not shown).

Specificity of Antibodies Raised against Different Domains of Myosin VI

The amino acid sequences of the myosins in each class are very conserved in different vertebrate species and it is usually the case that antibodies for a myosin from one species will cross-react with the same myosin in others. Antibodies were raised against different domains of chicken intestinal brush border myosin VI (shown schematically in Fig. 2 *a*) and affinity purified on GST- or His-tagged myosin VI fusion proteins. After affinity purification each of the antibodies recognized myosin VI on immunoblots of NRK and A431 fibroblasts. The predicted globular tail antibody (ab [PGT]) which was subsequently used for immunofluorescence reacted with a single band of the predicted molecular mass of 148 kD (Fig. 2 *b*). In NRK cells this antibody also recognized a band of lower molecular mass, which was probably a degradation product, since it varied between preparations. The tail ab (PGT) recognized myosin VI on immunoblots and also the native protein in whole cell extracts as shown by immunoprecipitation (Fig. 2 *c*). For specific, high yield immunoprecipitation of myosin VI, the whole tail ab (T) was found to be most effective. Immunoprecipitates of myosin VI from A431 cells with the tail antibodies (PGT and T) did not coprecipitate other myosins (Fig. 2 *d*).

Localization of Myosin VI in Fibroblasts

Using the tail ab (PGT) on NRK cells, myosin VI was observed by indirect immunofluorescence to show a dual localization (Fig. 3, *a* and *b*) at the leading edge and in the juxtanuclear area. There was also a considerable amount

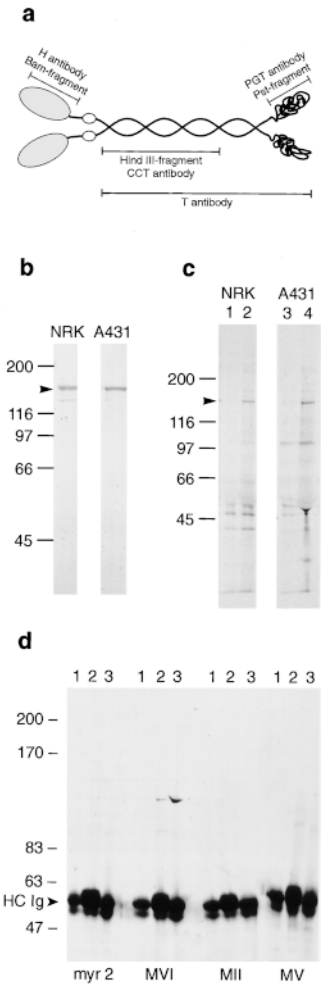

Figure 2. Specificity of the myosin VI tail antibody (PGT). (*a*) Schematic diagram of the structure of myosin VI showing the different domains which were expressed in *E. coli* as GST-fusion proteins and used to raise antibodies. A BamHI fragment encoding aa 308–631 of the head domain was used to raise the H ab; a HindIII fragment of the myosin VI tail encoding aa 742–1,030 was used to raise the CCT ab, a PstI fragment encoding the COOH-terminal globular tail was used to raise the PGT ab and an ab was raised against the whole tail (T ab) encoding aa 846–1,254. (*b*) Immunoblot of whole cell extracts of NRK and A431 cells showing the specificity of the affinity purified PGT ab. (*c*) Immunoprecipitation of myosin VI from [^{35}S]methionine/cysteine-labeled NRK and A431 cells. Lanes *1* and *3* show immunoprecipitations using the preimmune serum, whereas for lanes *2* and *4*, 10 μg of the affinity purified PGT ab was used. (*d*) Immunoblot of immunoprecipitations from A431 cells of myosin VI probed with antibodies to different myosins. Lane *1*, immunoprecipitation using the preimmune serum; lane *2*, with the tail ab (PGT) to myosin VI; lane *3*, with the tail ab (T) to myosin VI. The immunoprecipitates were blotted onto nitrocellulose and probed with the polyclonal antibodies to myosin I (*myr2*), myosin VI (*MVI*), myosin II (*MII*), and myosin V (*MV*).

of myosin VI present as a cytosolic pool presumably reflecting the fact that this myosin shuttles between actin/membrane bound and soluble pools. Myosin VI was localized by immunoelectron microscopy on ultrathin frozen sections of NRK cells, using the tail ab (PGT) followed by protein A–gold (Fig. 3, *c–e*), which showed that it was enriched at the plasma membrane in regions with a highly dynamic appearance. For example, in Fig. 3 *c* the plasma membrane profile showing many protrusions at the top of the cell has a higher concentration of myosin VI than the smooth plasma membrane profile at the bottom of the cell. Myosin VI was found to be particularly enriched at the tips of filopodia, microvilli and also in ruffles (Fig. 3, *d* and *e*). Such membrane ruffles extend from the cell surface, as seen in Fig. 3, *d* and *e*, and may close up to form endocytic macropinosomes after touching another ruffle or falling back onto the cell surface. In cross section such newly formed macropinosomes in the NRK cells appeared heavily labeled with anti-myosin VI. Quantitation of the

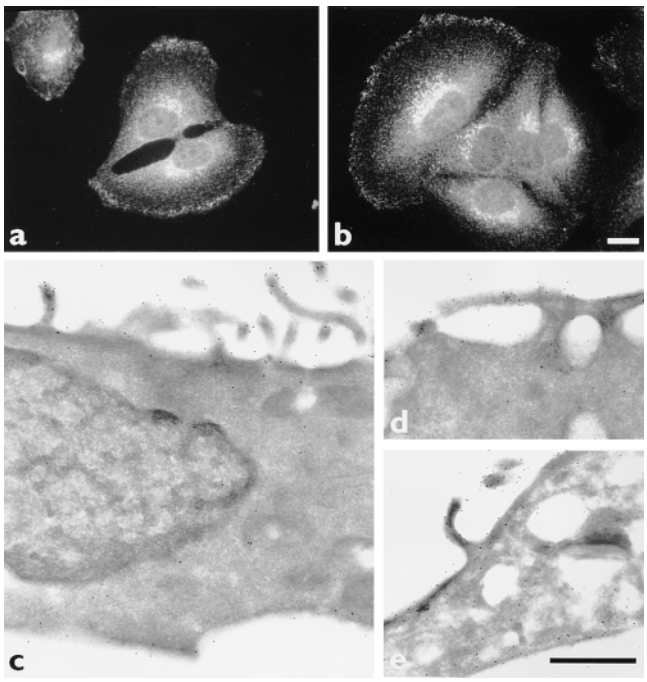

Figure 3. Localization of myosin VI in NRK cells. (*a* and *b*) Indirect immunofluorescence localization of myosin VI using the affinity purified tail ab (PGT) at 10 μg/ml. Myosin VI is especially enriched in the juxtanuclear area and in the dynamic leading edge of the fibroblast. There is also a cytosolic pool. (*c–e*) Immunoelectron microscopic localization of myosin VI on frozen thin sections with affinity purified tail ab (PGT) followed by protein A–gold. The highest concentration of myosin VI is visible at plasma membrane profiles with dynamic membrane protrusions. Bars: (*b*) 20 μm; (*e*) 500 nm.

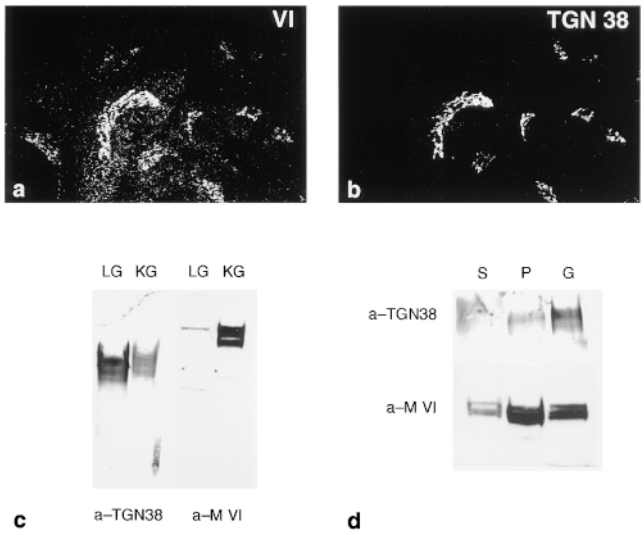

Figure 4. Association of myosin VI with the Golgi complex. NRK cells were double labeled by incubation with the affinity purified tail ab (PGT) (*a*) together with an mAb to TGN38 (*b*). Extended focus projections of a z-series of images obtained by confocal microscopy are shown. (*c*) Immunoblot of 15 μg of purified rat liver Golgi membranes (*LG*) or rat kidney Golgi membranes (*KG*) probed with antibodies to TGN38 or myosin VI. (*d*) Immunoblot of rat kidney factions. 10 μg each of cytosol (*S*, 100,000 *g*, 60 min supernatant), pellet (*P*, 100,000 *g*, 60 min pellet) and purified rat kidney Golgi membranes (*G*) were probed with the antibodies to TGN38 or myosin VI.

amount of myosin VI on unruffled plasma membrane compared with membrane protrusions revealed more than double the amount of myosin VI in areas with active membrane protrusions. We counted a total of 512 gold particles on 180 μm of unruffled plasma membrane i.e., 2.8 gold particles/μm of membrane and 884 gold particles on 120 μm of membrane protrusions i.e., 7.4 gold particles/μm of membrane. It was difficult to show specific labeling of myosin VI in the juxtanuclear area by EM, because of the high amount of myosin VI present as a cytosolic pool.

The Juxtanuclear Pool of Myosin VI

To investigate the juxtanuclear pool of myosin VI, NRK cells were double labeled for immunofluorescence and myosin VI was shown to colocalize with the trans Golgi network marker TGN 38 (Fig. 4, *a* and *b*). Colocalization with other Golgi markers (GM130 for the *cis*-Golgi, mannosidase II for the medial Golgi and galactosyltransferase for the *trans*-Golgi network [TGN]) was also observed (data not shown) consistent with myosin VI being present in the Golgi complex and the TGN.

To further test the association of myosin VI with isolated Golgi membranes, we purified Golgi complexes from rat kidney, since there is little myosin VI present in liver (Hasson and Mooseker, 1994). Our purified liver and kidney Golgi fractions contained similar amounts of the TGN marker TGN38 (Fig. 4 *c*) but only very small amounts of myosin VI could be found in the liver Golgi fraction compared with that from kidney (Fig. 4 *c*). Fractionation of a kidney homogenate into a 100,000 *g* supernatant and pellet showed that most of the myosin VI was found in the microsomal pellet and only small amounts remained in the cytosol (Fig. 4 *d*). A substantial proportion of the myosin VI was associated with the Golgi fraction. (Fig. 4 *d*). The same fractions were blotted for TGN38 which was predominantly enriched in the Golgi fraction, with some in the microsomal pellet and none in the soluble cytosolic fraction (Fig. 4 *d*).

Recruitment of Myosin V and VI into Surface Ruffles of A431 Cells after EGF Stimulation

The observed localization of myosin VI in the leading edge of fibroblasts suggested a functional role in the dynamic formation of ruffles and other membrane protrusions at the plasma membrane. In human carcinoma A431 cells this ruffling can be induced by the addition of EGF (Chinkers et al., 1979), and since these cells contain a high number of surface receptors for this growth factor, the ruffling response is very fast and dramatic. Ruffling requires an intact actin cytoskeleton and after the addition of EGF, the actin-membrane linking protein ezrin becomes phosphorylated and is recruited into microvilli/filopodia and the newly formed ruffles (Bretscher 1989). As shown in Fig. 5 we found that in unstimulated cells, ezrin showed a uniform cytosolic distribution with no particular localiza-

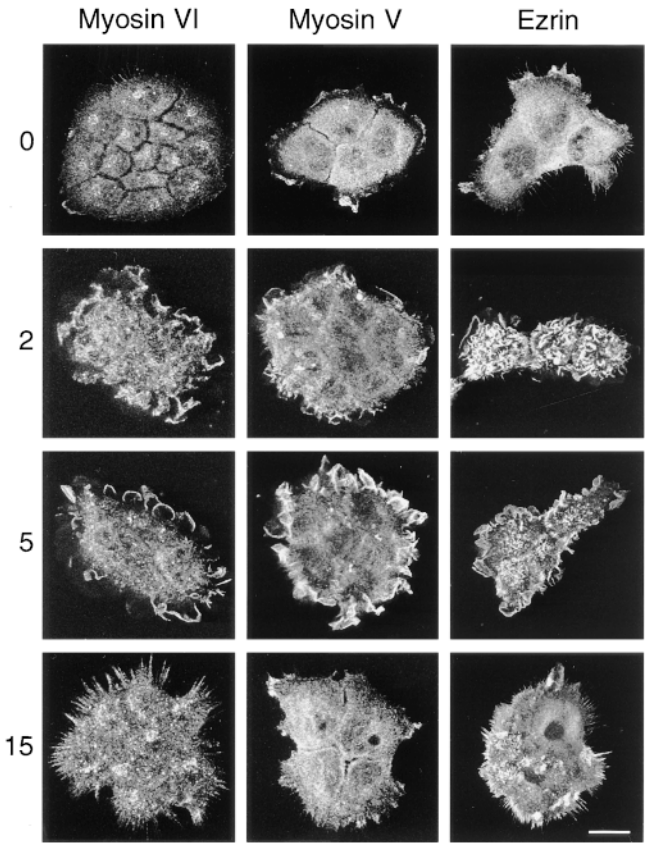

Figure 5. Localization of myosin VI, V, and ezrin in A431 cells after stimulation with EGF. Cells were fixed at 0, 2, 5, and 15 min after addition of EGF and stained with rabbit polyclonal antibodies to myosin VI (affinity-purified PGT ab), myosin V (affinity-purified tail domain ab), and ezrin (affinity-purified ab) followed by fluorescently labeled anti–rabbit IgG. Extended focus projections of a z-series of images obtained by confocal microscopy are shown. Bar, 20 μm.

tion, but 2 min after EGF stimulation, ezrin became concentrated in small ruffles and microvilli-like structures covering the entire surface of the cell. Some minutes later (5–10 min) ruffling reached its peak around the edge of the cell, where ezrin became concentrated. After 15 min, the cells rounded up and ezrin was observed in the retraction fibers and in a very fine punctate pattern below the plasma membrane on the upper surface of the cells. We used the tail ab (PGT) to examine the involvement of myosin VI in the response of A431 cells to EGF. Since myosin V has been implicated in the transport of membrane vesicles along actin fibres to cellular extensions (reviewed in Titus, 1997) and has been shown to be involved in regulation of filopodia extensions from neuronal cell growth cones (Wang et al., 1996) we also examined its recruitment into ruffles of A431 cells using a specific antibody. In unstimulated cells, both myosins showed a cytosolic distribution with the myosin V being slightly enriched in preexisting small surface ruffles and myosin VI being concentrated in the juxtanuclear region. After EGF stimulation for 2 min, unlike ezrin, myosin V and VI were not recruited into surface structures on top of the cells, but along with ezrin they became very concentrated in the ruffles at the edge of the cell after 5 min stimulation. After 15 min stimulation with EGF, myosin VI was present in the contraction fibers, whereas myosin V displayed a more even distribution throughout the cell.

Phosphorylation of Myosin VI after EGF Stimulation

To investigate whether myosin VI like ezrin (Bretscher, 1989) was phosphorylated in vivo in A431 cells after stimulation with EGF we labeled cells with [^{33}P]phosphate. After stimulation there was a clear increase in the level of phosphorylation of both myosin VI and ezrin (Fig. 6 *a*). We examined the time course of phosphorylation of myosin VI and ezrin after EGF stimulation and found that myosin VI was not as rapidly phosphorylated as ezrin but after 15 min the same increase in stimulation of phosphorylation was observed (Fig. 6 *b*). The slower increase in the rate of myosin VI phosphorylation was consistent with its slower recruitment into ruffles compared with phosphorylated ezrin (Fig. 5). Comparing the intensities of the radioactive bands on the autoradiogram with the Coomassie stained bands of myosin VI and ezrin on the gels suggested that the maximum level of phosphorylation of myosin VI was similar to that of ezrin.

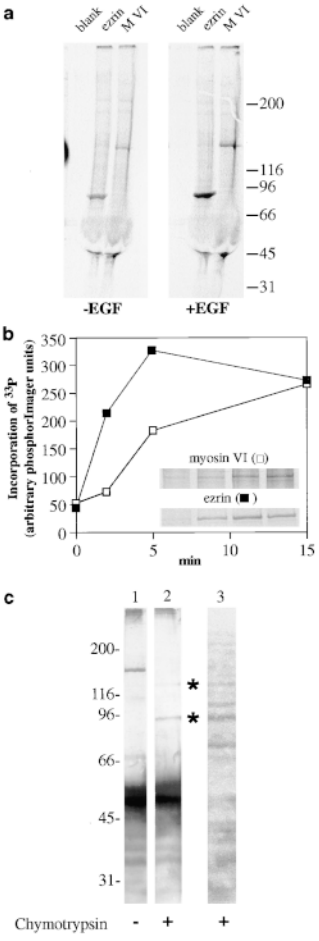

Figure 6. Phosphorylation of myosin VI in vivo. (*a*) A431 cells were first labeled with ^{33}P for 1 h and then used unstimulated or were stimulated with EGF before immunoprecipitation of myosin VI and ezrin. Phosphorylation of myosin VI and ezrin increased after stimulation with EGF. (*b*) Time course of phosphorylation of myosin VI and ezrin in A431 cells after stimulation with EGF. ^{33}P-labeled cells were stimulated before lysing the cells for immunoprecipitation with antibodies to myosin VI or ezrin after 2, 5, or 15 min. The amount of ^{33}P incorporation into ezrin (■) or myosin VI (□) was quantified using a phosphorImager and plotted as a function of time. (*c*) Chymotryptic digest of ^{33}P-phosphorylated myosin VI. The ^{33}P-labeled myosin VI was immunoprecipitated from A431 cells and digested with chymotrypsin before blotting with the antibody to the head domain of myosin VI, lanes *1* and *2*. Lane *3* shows the autoradiogram of the blot shown in lane *2*. An asterisk marks the bands recognized by the ab to the head domain (H) in lane *2* and also labeled with ^{33}P (lane *3*), indicating that phosphorylation of myosin VI occurs in the head domain.

Myosin VIs are the only class of myosins in higher multicellular organisms which have so far been shown to contain a putative heavy chain phosphorylation site similar to that found in the motor domains of *Acanthamoeba* and *Dictyostelium* myosin Is (Brzeska and Korn, 1996). To investigate the site of phosphorylation of myosin VI after EGF stimulation of A431 cells, immunoprecipitated ^{33}P-labeled myosin VI was partially digested with chymotrypsin under native conditions and fragments containing the head domain identified by immuno-blotting with the head antibody (H). Chymotrypsin was used under conditions where it has previously been shown to yield a relatively intact motor domain in skeletal, smooth muscle, and cytoplasmic myosin IIs. Fig. 6 *c* shows that two fragments containing the head domain were the major phosphorylated products of chymotryptic digestion of myosin VI from A431 cells.

Phosphorylation of Myosin VI by PAK In Vitro

The motor domain (heavy chain) of amoeboid myosin Is is phosphorylated by specific myosin I heavy chain kinases (MIHCK). Since these MIHCKs have recently been shown to be homologous to the mammalian PAK (Brzeska and Korn, 1996; Sells and Chernoff, 1997) we tested whether the myosin VI from A431 cells could be phosphorylated by PAK. Myosin VI and a mammalian myosin I (myr 2; Ruppert et al., 1995), as a control, were therefore immunoprecipitated from A431 cells and incubated with activated recombinant GST-PAK in the presence of γ-[^{32}P]ATP. PAK clearly phosphorylates the myosin VI (MVI) but not the myosin I (myr 2; Fig. 7 *a*). The PAK was also able to phosphorylate, in vitro, a recombinant myosin VI head fragment (aa 308–631) bacterially expressed as a GST fusion protein. This fragment contains the predicted MIHCK/PAK phosphorylation site at threonine residue 406. Under the same conditions, bacterially expressed GST and purified subfragment 1 from smooth muscle myosin II were not phosphorylated (Fig. 7 *b*). Interestingly the regulatory light chain of smooth muscle myosin II was phosphorylated under these conditions.

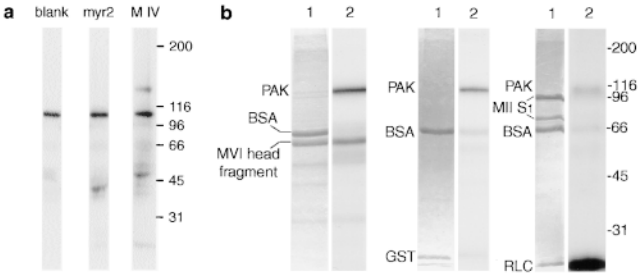

Figure 7. Phosphorylation in vitro by PAK. (*a*) Myosin VI and myosin I (*myr 2*) were immunoprecipitated from A431 cells and then incubated with recombinant GST-PAK and γ-[^{32}P]ATP for 30 min. Myosin VI (148 kD) but not myosin I (*myr 2*, 118 kD) was clearly phosphorylated by PAK, which also autophosphorylates and results in a band at 105 kD (*b*). Myosin VI head fragment (aa 308–631) was expressed in *E. coli* as a GST-fusion protein, purified and incubated with recombinant GST-PAK and γ-[^{32}P]ATP for 30 min. As controls bacterially expressed GST or the motor domain (subfragment 1) of smooth muscle myosin II (*MII S1*) were incubated with PAK. The major heavy chain fragment in the smooth muscle myosin subfragment 1 runs at 90 kD with a minor heavy chain fragment at 70 kD. Lane *1* shows the Coomassie stained gel and lane *2* the corresponding autoradiogram of the same gel.

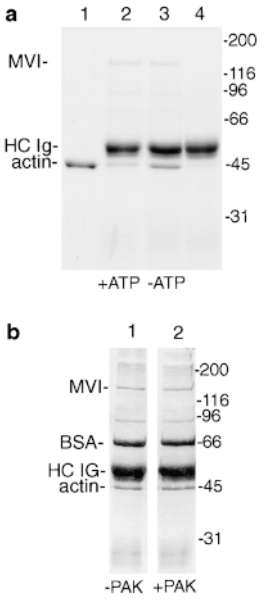

Figure 8. Binding of myosin VI to actin filaments. Myosin VI was immunoprecipitated from A431 cells under native conditions (*a*) and incubated with 10 μM of F-actin in the presence (lane *2*) or absence (lane *3*) of 2.5 mM MgATP. The immunobeads containing bound myosin VI were briefly centrifuged and washed with or without MgATP to remove nonbound actin. The washed beads were run on SDS-PAGE and stained with Coomassie blue. Lane *1* shows actin alone and lane *4* an immunoprecipitation with preimmune serum incubated with actin. In *b* the immunoprecipitated myosin VI was incubated with (lane *2*) or without (lane *1*) recombinant PAK before assessing binding to actin filaments under the same conditions as described in *a*.

Does Phosphorylation Affect Actin Binding?

Myosin VI from A431 cells, immunocaptured on a bead support, bound to F-actin in the absence of MgATP (rigor binding) and binding was significantly decreased (8–10-fold lower) in the presence of MgATP (Fig. 8 *a*). When the myosin VI was first phosphorylated in vitro by PAK there was no significant effect on its ability to bind actin in the presence of MgATP (Fig. 8 *b*). These results are in agreement with previous observations in *Acanthamoeba* myosin I where phosphorylation in the head domain leads to an increase in the actin-activated myosin I MgATPase activity (Maruta and Korn, 1977).

Discussion

Isoforms of Myosin VI

We have cloned and sequenced a full-length cDNA encoding a chicken intestinal brush border myosin VI and used antibodies to bacterially expressed fragments of this myosin to determine its intracellular localization in NRK and A431 cells. In *Drosophila*, two isoforms of myosin VI have been described, one being alternatively spliced and having an additional 15 aa inserted at the end of the coiled coil domain just before the predicted globular tail (Kellerman and Miller, 1992). The chicken cDNA that we isolated encodes a myosin VI (myosin VI B) most similar to the alternatively spliced *Drosophila* isoform, but with a 23-aa insert rather than a 15-aa insert at the end of the predicted coiled coil domain. In vertebrate tissues immunoblotting has revealed two isoforms of myosin VI in frog hair cells (Hasson et al., 1997) and in NRK and Caco-2 cells (our un-

published data). In frogs the larger isoform is found predominantly in hair cell bundles, whereas the smaller isoform is found in all tissues (Hasson et al., 1997). The functions of the two isoforms are not known and their localization within individual cells has not yet been described.

Structure and Function of Myosin VI

Examining the chicken brush border myosin VI B sequence reveals several unique features which are not found in the other vertebrate myosin classes and which may contribute to its specific function as a motor protein involved in membrane traffic. In the motor domain there is a 22-aa insertion (residues 276–297 in Fig. 1) predicted to be in an exposed surface loop in the region between the ATP binding site and the upper 50-kD subdomain (Rayment et al., 1993; Cope et al., 1996). Also in the motor domain, myosin VI contains a threonine residue (T_{406}) within a conserved stretch of sequence (Bement and Mooseker, 1995) which in amoeboid myosin Is is phosphorylated by a specific heavy chain kinase and is involved in regulating amoeboid myosin I function (Maruta and Korn, 1977). Recently it was discovered that this MIHCK belongs to a family of Cdc 42/Rac regulated protein kinases that includes the mammalian PAK and the yeast STE20p and Cla4p kinases (reviewed by Brzeska and Korn, 1996). It should be noted that of unconventional myosins described so far in higher multicellular organisms only myosin VIs contain a similar putative phosphorylation site to that in amoeboid myosin Is. Our present data (*a*) provide the first demonstration that an unconventional myosin heavy chain in mammalian cells can be phosphorylated in vivo, (*b*) show that a major phosphorylation site is in the head domain, and (*c*) demonstrate that this myosin can be phosphorylated by p21 (Rac) activated protein kinase (PAK) in the motor domain. Interestingly the putative PAK phosphorylation site T_{406} is predicted to be in a surface loop between the upper and lower 50-kD subdomains in the region believed to be the actin binding interface. We have shown that PAK-mediated phosphorylation does not significantly affect myosin VI binding to actin. However, it remains possible that the phosphorylation event could control the duty cycle of myosin VI so that it remains attached to actin for a relatively long time thus allowing it to work as a processive motor with a larger duty ratio (i.e., the fraction of the myosin ATPase cycle that is spent strongly bound to actin and developing force). The neck region of myosin VI contains only one IQ motif unlike myosins I and V which have three to six IQ motifs and thus myosin VI appears to have a short lever arm. At first sight, this appears to be at odds with its proposed role in vesicular movement since the longer lever arms of myosins I and V have been proposed to result in an increased working stroke consistent with their involvement in membrane traffic (Howard, 1997). However, in between the motor domain and the IQ motif of myosin VI there is a spacer region which has no apparent structural motifs and therefore may be flexible and could perhaps function like the neck region in the kinesins.

Two coiled-coil regions are predicted to be present in the tail of the molecule. Whereas the first domain is probably a correct prediction, and could be involved in the dimerization of the molecule, the second region seems unlikely to be correct. This region is very highly charged and contains few hydrophobic residues, and there is little sign of a strong heptad periodicity. Instead there are repeats of charged residues, in the form of alternating blocks of four acidic and four basic residues. We suggest that such a highly charged sequence is likely to be fully exposed to the solvent and to form a helix which is stabilized by interactions between the alternating charges along it. Perhaps this region acts as an extended linker region involved in protein–protein interactions and therefore serves as a specific recognition site.

The extreme COOH-terminal domain is the most highly conserved region in all the myosin VIs so far sequenced. It is unique to myosin VI and is predicted to form a globular domain; therefore it is an excellent candidate domain for interaction with specific membrane receptors and/or defining the cellular function of this unconventional myosin.

Intracellular Localization of Myosin VI

Polyclonal antibodies raised against the predicted globular COOH-terminal tail domain (PGT) reacted specifically with myosin VI in immunoblotting and immunoprecipitation experiments, and since to date, information on the intracellular distribution of myosin VI has been sparse these antibodies were used to study the localization of this myosin by immunofluorescence and immuno EM in NRK and A431 cells. It was found that in these cells, myosin VI was associated with the Golgi complex and the leading, ruffling edge of the cell as well as being present in a cytosolic pool. We have not examined further the functional role of the Golgi associated part of myosin VI. The localization of myosin I (Fath and Burgess, 1993; Fath et al., 1994) and myosin II (de Almeida et al., 1993; Ikonen et al., 1997) in the Golgi complex has led to much speculation about the role of myosins in this organelle. Myosin II has been suggested to play a role in the production of constitutive transport vesicles from the TGN (Müsch et al., 1997), but recently some of these results have been questioned by the observation that the mAb used in these studies also cross reacts with βCOP (Simon et al., 1998). The fact that inhibition of myosin ATPase activity with BDM prevents production of transport vesicles from the TGN (Müsch et al., 1997) remains consistent with a role for myosin in this process.

Myosin VI and Ruffling

The plasma membrane at the leading edge of a cultured cell exhibits a highly mobile behavior. The shape of the cell surface is constantly changing with ruffles, filopodia and lamellipodia being formed and a large number of exocytic and/or endocytic vesicles being translocated. Since the actin cytoskeleton is concentrated beneath the plasma membrane and microtubules do not extend to the cell surface, actin based motor proteins must be used to generate the force and movement in the cortical actin network. A myosin I isoform is known to be localized in motile areas including filopodia, lamellipodia, and growth cones (Wagner et al., 1992). Regulation of filopodia extensions from

growth cones during neuronal development has also been shown to be dependent on myosin V (Wang et al., 1996). Our studies indicate that myosin VI is also present in membrane ruffles and filopodia protruding from the plasma membrane. Our demonstration that recruitment of myosin VI into surface ruffles is accompanied by an increase in its phosphorylation in the head domain is an exciting new finding. Furthermore we have shown that PAK phosphorylates myosin VI and the bacterially expressed head domain in vitro, suggesting it is a candidate for this function in vivo. Since in the amoeboid myosin I's phosphorylation by the PAK homologue MIHCK is required for switching on acto-myosin ATPase activity, it is likely that phosphorylation in myosin VI also leads to an increase in ATPase activity and cytoskeletal dynamics. PAK has previously been linked to membrane ruffling since microinjection of activated PAK into quiescent fibroblasts induced the rapid formation of filopodia and membrane ruffles (Sells et al., 1997). This kinase is also known to bind and become activated by the GTP-bound (activated) form of Rac (Manser et al., 1994). Thus, we can envisage a signaling pathway whereby the EGF receptor is linked to the actin cytoskeleton and membrane ruffling via activation of phosphatidylinositol 3-kinase, Rac, PAK, and phosphorylation of myosin VI. However, the function of myosin VI in these surface structures has not yet been resolved. It could be involved in generating the protrusive force in the tip of a membrane extension by moving towards the barbed end of the actin filament while remaining bound to the plasma membrane probably via a receptor (for review Mitchison and Cramer, 1996). The region of the plasma membrane forming a ruffle or filopodium appears to be very flexible and acto-myosin interactions may be involved in generating either bending or pulling forces, which enable circular surface ruffles to form (Dowrick et al., 1993). Such ruffles can close allowing the formation of macropinosomes (Swanson and Watts, 1995). The whole process of macropinocytosis that takes place at cell margins within the actin-rich ruffling surfaces, may be dependent on motor proteins like myosin V and VI. Furthermore internalized macropinosomes and also other endocytic vesicles could be transported through the dense cortical actin network along actin filaments with the help of these myosin motors. The dual localization of myosin VI to the Golgi complex and the dynamic, ruffling leading edge of fibroblastic cells also suggests a direct involvement in exocytic membrane transport from the Golgi complex to the leading edge.

We thank Margaret Robinson, Nick Bright, Tony Hodge, and Barbara Reaves for much valuable discussion.

This work was funded by the Medical Research Council. C. Lionne was in receipt of an European Molecular Biology Organization long-term fellowship.

Received for publication 8 December 1997 and in revised form 20 October 1998.

References

Allan, V. 1996. Role of motor proteins in organizing the endoplasmic reticulum and Golgi apparatus. *Semin. Cell Devel. Biol.* 7:335–342.

Avraham, K.B., T. Hasson, K.P. Steel, D.M. Kingsley, L.B. Russell, M.S. Mooseker, N.G. Copeland, and N.A. Jenkins. 1995. The mouse *Snell's waltzer* deafness gene encodes an unconventional myosin required for structural integrity of inner ear hair cells. *Nat. Genet.* 11:369–375.

Ayscough, K.R., J. Stryker, N. Pokala, M. Sanders, P. Crews, and D.G. Drubin. 1997. High rates of actin filament turnover in budding yeast and roles for actin in establishment and maintenance of cell polarity revealed using the actin inhibitor latrunculin-A. *J. Cell Biol.* 137:399–416.

Beck, K.A., J.A. Burchanan, V. Malhotra, and W.J. Nelson. 1994. Golgi spectrin: identification of an erythroid β-spectrin homolog associated with the Golgi complex. *J. Cell Biol.* 127:707–723.

Bement, W.M., T. Hasson, J.A. Wirth, R.E. Cheney, and M.S. Mooseker. 1994. Identification and overlapping expression of multiple unconventional myosin genes in vertebrate cell types. *Proc. Natl. Acad. Sci. USA.* 91:6549–6553.

Bement, W.M., and M.S. Mooseker. 1995. TEDS rule: a molecular rationale for differentional regulation of myosins by phosphorylation of the heavy chain head. *Cell. Motil. Cytoskeleton.* 31:87–92.

Berger, B., D.B. Wilson, E. Wolf, T. Tonchev, M. Milla, and P.S. Kim. 1995. Predicting coiled coils by use of pairwise residue correlations. *Proc. Natl. Acad. Sci. USA.* 92:8259–8263.

Bretscher, A. 1989. Rapid phosphorylation and reorganization of ezrin and spectrin accompany morphological changes induced in A-431 cells by epidermal growth factor. *J. Cell Biol.* 108:921–930.

Brzeska, H., and E.D. Korn. 1996. Regulation of class I and class II myosins by heavy chain phosphorylation. *J. Biol. Chem.* 271:16983–16986.

Chinkers, M., J.A. McKanna, and S. Cohen. 1979. Rapid induction of morphological changes in human carcinoma cells A-431 by epidermal growth factor. *J. Cell Biol.* 83:260–265.

Cole, N.B., and J. Lippincott-Schwartz. 1995. Organization of organelles and membrane traffic by microtubules. *Curr. Opin. Cell Biol.* 7:55–64.

Cope, M.J.T.V., J. Whisstock, I. Rayment, and J. Kendrick-Jones. 1996. Conservation within the myosin motor domain: implications for structure and function. *Structure.* 4:969–987.

de Almeida, J.B., J. Doherty, D.A. Ausiello, and J.L. Stow. 1993. Binding of the cytosolic p200 protein to Golgi membranes is regulated by heterotrimeric G proteins. *J. Cell Sci.* 106:1239–1248.

Dowrick, P., P. Kenworthy, B. McCann, and R Warn. 1993. Circular ruffle formation and closure lead to macropinocytosis in hepatocyte growth factor/scatter factor-treated cells. *Eur. J. Cell Biol.* 61:44–53.

Durrbach, A., D. Louvard, and E. Coudrier. 1996. Actin filaments facilitate two steps of endocytosis. *J. Cell Sci.* 109:457–465.

Fath, K.R., and D.R. Burgess. 1993. Golgi-derived vesicles from developing epithelial cells bind actin filaments and possess myosin-I as a cytoplasmically oriented peripheral membrane protein. *J. Cell Biol.* 120:117–127.

Fath, K.R., G.M. Trimbur, and D.R. Burgess. 1994. Molecular motors are differentially distributed on Golgi membranes from polarized epithelial cells. *J. Cell Biol.* 126:661–675.

Goodson, H.V., C. Valetti, and T.E. Kreis. 1997. Motors and membrane traffic. *Curr. Opin. Cell Biol.* 9:18–28.

Gottlieb, T.A., I.E. Ivanov, M. Adesnik, and D.D. Sabatini. 1993. Actin microfilaments play a critical role in endocytosis at the apical but not the basolateral surface of polarized epithelial cells. *J. Cell Biol.* 120:695–710.

Greenberg, A., J. El Kohoury, F. Di Virgilio, E.M. Kaplan, and S.C. Silverstein. 1991. Ca^{2+}-independent F-actin assembly and disassembly during Fc receptor-mediated phagocytosis in mouse macrophages. *J. Cell Biol.* 113:757–767.

Griffiths, G. 1993. Fine structure immunocytochemistry. Springer Verlag, Berlin. 1–459.

Griffiths, G., and H. Hoppeler. 1986. Quantitation in immunocytochemistry, correlation of immunogold labelling to absolute number of membrane antigens. *J. Histochem. Cytochem.* 34:1389–1398.

Harlow, E., and D. Lane. 1988. Antibodies: A Laboratory Manual. Cold Spring Harbor Laboratory, Cold Spring Harbor, NY. 726 pp.

Hasson, T., and M.S. Mooseker. 1994. Porcine myosin VI: characterization of a new mammalian unconventional myosin. *J. Cell Biol.* 127:425–440.

Hasson, T., and M.S. Mooseker. 1995. Molecular motors, membrane movements and physiology: emerging roles for myosins. *Curr. Opin. Cell Biol.* 7:587–594.

Hasson, T., P.G. Gillespie, J.A. Garcia, R.B. MacDonald, Y. Zhao, A.G. Yee, M.S. Mooseker, and D.P. Corey. 1997. Unconventional myosins in inner-ear sensory epithelia. *J. Cell Biol.* 137:1287–1307.

Heintzelman, M.B., T. Hasson, and M.S. Mooseker. 1994. Multiple unconventional myosin domains of the intestinal brush border cytoskeleton. *J. Cell Sci.* 107:3535–3543.

Hoock, T.C., L.L. Peters, and S.E. Lux. 1997. Isoforms of ankyrin-3 that lack the NH2-terminal repeats associate with mouse macrophage lysosomes. *J. Cell Biol.* 136:1059–1070.

Howard, J. 1997. Molecular motors: structural adaptations to cellular functions. *Nature.* 389:561–567.

Ikonen, E., J.B. de Almeid, K.L. Fath, D.R. Burgess, K. Ashman, K. Simons, and J.L. Stow. 1997. Myosin II is associated with Golgi membranes: identification of p200 as nonmuscle myosin II on Golgi-derived vesicles. *J. Cell Sci.* 110:2155–2164.

Jackman, M.R., W. Shurety, J.A. Ellis, and J.P. Luzio. 1994. Inhibition of apical but not basolateral endocytosis of ricin and folate in Caco-2 cells by cytochalasin D. *J. Cell Sci.* 107:2547–2556.

Kellerman, K.A., and K.G. Miller. 1992. An unconventional myosin heavy chain gene from *Drosophila melanogaster*. *J. Cell Biol.* 119:823–834.

Kneller, D.G., F.E. Cohen, and R. Langridge. 1990. Improvements in protein

secondary structure prediction by an enhanced neural network. *J. Mol. Biol.* 214:171–182.

Knight, A.E., and J. Kendrick-Jones. 1993. A myosin-like protein from a higher plant. *J. Mol. Biol.* 231:1–7.

Kubler, E., and H. Riezman. 1993. Actin and fimbrin are required for the internalization step of endocytosis in yeast. *EMBO (Eur. Mol. Biol. Organ.) J.* 12: 2855–2862.

Kyhse-Anderson, J. 1984. Electroblotting of multiple gels: a simple apparatus without buffer tank for rapid transfer of proteins from polyacrylamide to nitrocellulose. *J. Biochem. Biophys. Methods.* 10:203–209.

Lamaze, C., L.M. Fujimoto, H.L. Yin, and S.L. Schmid. 1997. The actin cytoskeleton is required for receptor-mediated endocytosis in mammalian cells. *J. Biol. Chem.* 272:20332–20335.

Lantz, V.A., and K.G. Miller. 1998. A class VI unconventional myosin is associated with a homologue of a microtubule-binding protein, cytoplasmic linker protein-170, in neurons and at the posterior pole of *Drosophila* embryos. *J. Cell Biol.* 140:897–910.

Li, G., E. Rungger-Brandle, I. Just, J.-C. Jonas, K. Aktories, and C.B. Wollheim. 1994. Effect of disruption of actin filaments by Clostridium botulinum C2 toxin on insulin secretion by HIT-T15 cells and pancreatic islets. *Mol. Biol. Cell.* 5:1199–1213.

Lupas, A., M. Van Dyke, and J. Stock. 1991. Predicting coiled coils from protein sequences. *Science.* 252:1162–1164.

Manser, E., T. Leung, H. Salihuddin, Z.S. Zhao, and L. Lim. 1994. A brain serine/threonine protein kinase activated by cdc42 and rac1. *Nature.* 367:40–46.

Maruta, H., and E.D. Korn. 1977. *Acanthamoeba* cofactor protein is a heavy chain kinase required for actin activation of the Mg^{2+}-ATPase activity of *Acanthamoeba* myosin I. *J. Biol. Chem.* 252:8329–8332.

Matsudiara, P., and D.R. Burgess. 1978. SDS microslab linear gradient PAGE. *Anal. Biochem.* 87:386–396.

Mermall, V., J.G. McNally, and K.G. Miller. 1994. Transport of cytoplasmic particles catalyzed by an unconventional myosin in living *Drosophila* embryos. *Nature.* 369:560–562.

Mermall, V., and K.G. Miller. 1995. The 95F unconventional myosin is required for proper organization of the *Drosophila* syncytial blastoderm. *J. Cell Biol.* 129:1575–1588.

Mermall, V., P.L. Post, and M.S. Mooseker. 1998. Unconventional myosins in cell movement, membrane traffic and signal transduction. *Science.* 279:527–533.

Mitchison, T.J., and L.P. Cramer. 1996. Actin-based cell motility and cell locomotion. *Cell.* 84:371–379.

Muallem, S., K. Kwiatkowska, X. Xu, and H.L. Yin. 1995. Actin filament disassembly is a sufficient final trigger for exocytosis in nonexcitable cells. *J. Cell Biol.* 128:589–598.

Murphy, C., R. Saffrich, M. Grummt, H. Gournier, V. Rybin, M. Rubino, P. Auvinen, A. Lütcke, R. Parton, and M. Zerial. 1996. Endosome dynamics regulated by a Rho protein. *Nature.* 384:427–432.

Müsch, A., D. Cohen, and E. Rodriguez-Boulan. 1997. Myosin II is involved in the production of constitutive transport vesicles from the TGN. *J. Cell Biol.* 138:291–306.

Nagai, K., and H.C. Thøgersen. 1987. Synthesis and sequence specific proteolysis of hybrid proteins produced in *E. coli*. *Methods Enzymol.* 153:461–481.

Novick, P., and D. Botstein. 1985. Phenotypic analysis of temperature sensitive yeast actin mutants. *Cell.* 40:405–415.

Orci, L., K.H. Gabbay, and W.J. Malaisse. 1972. Pancreatic beta-cell web: its possible role in insulin secretion. *Science.* 175:1128–1130.

Probst, F.J., R.A. Fridell, Y. Raphael, T.L. Saunders, A. Wang, Y. Liang, R.J. Morell, J.W. Touchman, R.H. Lyons, K. Noben-Trauth, et al. 1998. Correction of deafness in *shaker-2* mice by an unconventional myosin in a BAC Transgene. *Science.* 280:1444–1447.

Rayment, I., R.W. Rypniewski, K. Schmidt-Base, R. Smith, D.R. Tomchick, M.M. Benning, D.A. Winkelmann, G. Wessenberg, and H.M. Holden. 1993. Three-dimensional structure of myosin subfragment-1: a molecular motor. *Science.* 261:50–58.

Reaves, B.J., A.A. Bright, B.M. Mullock, and J.P. Luzio. 1996. The effect of wortmannin on the localization of lysosomal type I integral membrane glycoproteins suggests a role for phosphoinositide 3-kinase activity in regulating membrane traffic in the late endocytic pathway. *J. Cell Sci.* 109:749–762.

Ruppert, C., J. Godel, R.T. Müller, R. Kroschewski, J. Reinhard, and M. Bähler. 1995. Localization of the rat myosin I molecules myr 1 and myr 2 and in vivo targeting of their tail domains. *J. Cell Sci.* 108:3775–3786.

Sambrook, J., E.F. Fritsch, and T. Maniatis. 1989. Molecular Cloning: A Laboratory Manual. 2nd edition. Cold Spring Harbor Laboratory, Cold Spring Harbor, NY.

Sells, M.A., U.G. Knaus, S. Bagrodia, D.M. Ambrose, G.M. Bokoch, and J. Chernoff. 1997. Human p21-activated kinase (Pak1) regulates actin organization in mammalian cells. *Curr. Biol.* 7:202–210.

Sells, M.A., and J. Chernoff. 1997. Emerging from the Pak: the p21-activated protein kinase family. *Trends Cell Biol.* 7:162–167.

Shurety, W., N.A. Bright, and J.P. Luzio. 1996. The effects of cytochalasin D and phorbol myristate acetate on the apical endocytosis of ricin in polarized Caco-2 cells. *J. Cell Sci.* 109:2927–2935.

Simon, J.P., T.-H. Shen, I.E. Ivanov, D. Gravotta, T. Morimoto, M. Adesnik, and D.D. Sabatini. 1998. Coatomer, but not P200/myosin II, is required for the *in vitro* formation of *trans*-Golgi network derived vesicles containing the envelope glycoprotein of vesicular stomatitis virus. *Proc. Natl. Acad. Sci. USA.* 95:1073–1078.

Slusarewicz, P., N. Hui, and G. Warren. 1994. Purification of rat liver Golgi stacks. Cell Biology: A Laboratory Handbook. Academic Press, San Diego, CA. 509–524.

Studier, F.W., and B.A. Moffat. 1986. Use of bacteriophage T7 RNA polymerase to direct selective high-level expression of cloned genes. *J. Mol. Biol.* 189:113–130.

Swanson, J.A., and C. Watts. 1995. Macropinocytosis. *Trends Cell Biol.* 5:424–428.

Titus, M.A. 1997. Unconventional myosins: new frontiers in actin-based motors. *Trends Cell Biol.* 7:119–123.

van Deurs, B., P.K. Holm, L. Kaiser, and K. Sandvig. 1995. Delivery to lysosomes in human carcinoma cell line HEP-2 involves an actin filament-facilitated fusion between mature endosomes and preexisting lysosomes. *Eur. J. Cell Biol.* 66:309–323.

Wagner, M.C., B. Barylko, and J.P. Albanesi. 1992. Tissue distribution and subcellular localization of mammalian myosin I. *J. Cell Biol.* 119:163–170.

Wang, F.-S., J.S. Wolenski, R.E. Cheney, M.S. Mooseker, and D.G. Jay. 1996. Function of myosin-V in filopodial extension of neuronal growth cones. *Science.* 273:660–663.

Weiner, O.H., J. Murphy, G. Griffiths, M. Schleicher, and A.A. Noegel. 1993. The actin-binding protein comitin (p24) is a component of the Golgi apparatus. *J. Cell Biol.* 123:23–34.

Wu, C., S.-F. Lee, E. Furmaniak-Kazmierczak, G.P. Côté, D.Y. Thomas, and E. Leberer. 1996. Activation of myosin-I by members of the Ste20p protein kinase family. *J. Biol. Chem.* 271:31787–31790.